Published in final edited form as:
Stem Cells. 2011 August ; 29(8): 1283–1293. doi:10.1002/stem.680.

Novel Stem/Progenitor Cell Population from Murine Tracheal Submucosal Gland Ducts with Multipotent Regenerative Potential

Ahmed E. Hegab[a], **Vi Luan Ha**[a], **Jennifer L. Gilbert**[a], **Kelvin Xi Zhang**[b], **Stephen P. Malkoski**[c], **Andy T. Chon**[a], **Daphne O. Darmawan**[a], **Bharti Bisht**[a], **Aik T. Ooi**[a], **Matteo Pellegrini**[d], **Derek W. Nickerson**[a], and **Brigitte N. Gomperts**[a,e,f,g]

[a]Department of Pediatrics, David Geffen School of Medicine at University of California Los Angeles, University of California Los Angeles School of Medicine, Los Angeles, California, USA

[b]Department of Biological Chemistry, Howard Hughes Medical Institute, University of California Los Angeles, Los Angeles, California, USA

[c]Division of Pulmonary Sciences and Critical Care Medicine, University of Colorado Denver Health Sciences Center, Aurora, Colorado, USA

[d]Department of Molecular, Cellular, and Developmental Biology, University of California Los Angeles, Los Angeles, California, USA

[e]Jonsson Comprehensive Cancer Center, Los Angeles, California, USA

[f]Department of Medicine, Division of Pulmonary and Critical Care Medicine, David Geffen School of Medicine, University of California Los Angeles, Los Angeles, California, USA

[g]Eli and Edythe Broad Center of Regenerative Medicine and Stem Cell Research, University of California Los Angeles, Los Angeles, California, USA

Abstract

The airway epithelium is in direct contact with the environment and therefore constantly at risk for injury. Basal cells (BCs) have been found to repair the surface epithelium (SE), but the contribution of other stem cell populations to airway epithelial repair has not been identified. We demonstrated that airway submucosal gland (SMG) duct cells, in addition to BCs, survived severe hypoxic-ischemic injury. We developed a method to isolate duct cells from the airway. In vitro and in vivo models were used to compare the self-renewal and differentiation potential of duct cells and BCs. We found that only duct cells were capable of regenerating SMG tubules and ducts, as well as the SE overlying the SMGs. SMG duct cells are therefore a multipotent stem cell for airway epithelial repair This is of importance to the field of lung regeneration as determining the

Correspondence: Brigitte N. Gomperts, M.D., 10833 Le Conte Ave., A2-410 MDCC, Los Angeles, California 90095, USA. Telephone: 1-310-825-6708; Fax: 1-310-206-8089; bgomperts@mednet.ucla.edu.

Author contributions: A.E.H.: conception and design, collection and/or assembly of data, data analysis and interpretation, and manuscript writing; V.L.H., J.L.G., A.T.C., and D.O.D.: collection and/or assembly of data; K.X.Z., B.B., A.T.O., and M.P.: data analysis and interpretation; S.P.M.: provision of study material; D.W.N.: collection and/or assembly of data, data analysis and interpretation; B.N.G.: conception and design, collection and/or assembly of data, data analysis and interpretation, manuscript writing, and final approval of manuscript.

Disclosure of Potential Conflicts of Interest
There are no conflicts of interest.

See www.StemCells.com for supporting information available online.

repairing cell populations could lead to the identification of novel therapeutic targets and cell-based therapies for patients with airway diseases.

Keywords

Airway epithelial repair and regeneration; Lung stem cells; Submucosal glands; Hypoxic-ischemic injury

Introduction

The airway epithelial cells of the conducting airways perform an essential role in innate host defense both by providing a physical barrier and by producing mucus and serous secretions that allow the body to clear infectious agents and environmental toxins [1]. These airway epithelial cells are constantly at risk for injury as they are in direct contact with the environment. The ability of the airway surface epithelium (SE) to undergo efficient repair and functional regeneration is an important part of protection of the host.

The identity of all the resident stem or progenitor cells responsible for airway postnatal growth, homeostasis, and repair after injury remains under investigation [2–4]. Recently, lineage tracing and isolation of cell populations was used to provide compelling evidence that the majority of basal cells (BCs) in the trachea and Clara cells in the bronchi and bronchioles can self-renew and generate differentiated progeny of the SE [5, 6].

The airway SE consists of many cell types, which have defined locations and cell markers (Fig. 1). BCs are classically rounded cells with low pyramidal nuclei and express cytokeratin (K)5 and p63. Secretory cells (Clara and serous cells) are identified by their columnar shape and expression of secretoglobin1A1 (SCGB1A1) and the polymeric immunoglobulin receptor (pIgR), lysozyme, and/or lactoferrin. Ciliated cells are identified by their characteristic columnar shape and cilia that stain positively for acetylated tubulins. There are also a lesser number of neuroendocrine cells and a few goblet cells in the airway epithelium. The vast majority of mucus and serous secretions are produced by the submucosal glands (SMGs) that are present in the submucosal region of the airway between the SE and the cartilage rings (Fig. 1A). SMGs consist of interconnected serous and mucus tubules, which are lined by polyhedral serous and mucus cells with rounded basal nuclei. Mucus can be detected in mucus cells with Alcian Blue/periodic acid-Schiff (AB/PAS) staining and with deleted in malignant brain tumors 1 (DMBT1), while serous cells express lysozyme, lactoferrin, and pIgR. SMG tubules are surrounded by flat, thin myoepithelial cells (MECs), which express K5, K14, and α-smooth muscle actin (αSMA). Serous and mucus tubules converge into collecting ducts that turn into ciliated duct before opening into the SE [7]. SMG duct cells characteristically express K5 and K14.

In human lungs, SMGs exist along the airways from the larynx down to the distal part of the main bronchi. However, in mouse lungs, they are restricted to the upper trachea with the biggest bunch of glands being lodged between the cricoid cartilage and the first tracheal cartilaginous ring (C1) [8].

SMGs and SMG ducts lie below the SE in the submucosal region of the airway, which is a relatively protected anatomical location in comparison with the SE. Label-retaining cells have been found to localize to the SMG and its ducts [9]. The ducts of other glandular tissues, such as breast and salivary glands, have been found to harbor adult stem/progenitor cell populations, suggesting the possibility of an analogous epithelial stem/progenitor cell in the SMG duct [10, 11]. However, the potential contribution of SMG duct cells to airway epithelial repair has not been fully explored. The regenerative capacity of SMG duct cells is

not known, as no techniques have existed up until now to selectively isolate the SMG duct cells to evaluate their stem cell properties.

Here, we demonstrate the role of the SMG duct cell in regeneration of both the SMG tubules and the SE after severe hypoxic-ischemic injury. Using a novel method to isolate SMG duct cells from the airway, we use in vitro and in vivo stem cell model systems and lineage tracing to show that the SMG duct cells have the ability to self-renew and differentiate into SMGs and SMG duct cells as well as to form the SE adjacent to the submucosal duct area.

Materials and Methods

Mice

Wild-type C57BL/6, β-actin green fluorescent protein (GFP) (C57BL/6-Tg[ACTbEGFP]1Osb), β-actin red fluorescent protein (RFP) (C57BL/6-Tg[ACTbERFP]1Nagy/J), and ROSA26-flox-STOP-yellow fluorescent protein (YFP) (B6.129X1-Gt(ROSA)26Sor$^{t\text{-}m1(EYFP)Cos}$/J) mouse strains were purchased from The Jackson Laboratory (Bar Harbor, Maine, http://www.jax.org/). Transgenic C57/BL6 K14-CrePR1 mice were made and kindly provided by Xiao Jing Wang. Mice were housed and bred under the regulation of the Division of Laboratory Animal Medicine at the UCLA.

Mouse Tracheal Transplant Model

We used a well-established, reproducible murine model of tracheal epithelial regeneration using syngeneic subcutaneous tracheal transplantation from C57BL/6 into C57BL/6 mice [12, 13]. Tracheal grafts were collected from euthanized mice at post-transplant days 1 and 3, then formalin fixed and paraffin embedded.

In Vivo SMG Regeneration Model

Five thousand sorted duct cells were directly injected into the fat pad around the scapular region of the mouse back. At collection of the grafts, the whole fat pad was excised and sectioned.

Immunostaining

Longitudinally embedded tracheas were cut from paraffin blocks ensuring the inclusion of any existing SMGs from below the larynx to at least C10. Spheres and air-liquid interface (ALI) cultures were fixed in formalin, covered in Histogel (Fisher Scientific, Pittsburgh, PA, http://www.fishersci.com), and then paraffin embedded and sectioned. Immunostaining was performed as described [14]. The primary antibodies used were chicken K15, rabbit K5 and K14 (Covance, Princeton, NJ, www.covance.com), Mouse p63, goat K5, SCGB1A1 and DMBT1 (Santa Cruz, CA, www.scbt.com), rat integrin-α-6 (ITGA6), rabbit nerve growth factor receptor (NGFR), mouse and rabbit K14 (Abcam, Cambridge, MA, www.abcam.com), goat tumor-associated calcium signal transducer 2 (TROP-2) and pIgR (R&D, Minneapolis, MN, www.rndsystems.com), chicken K8 (Novus Biologicals, Littleton, CO, www.novusbio.com), rat epithelial cell adhesion molecule (EpCAM)-647 (Biolegends, San Diego, CA, www.biolegend.com), rabbit lactoferrin (Millipore, Billerica, MA, www.millipore.com/antibodies), goat GFP (Rockland, Gilbertsville, PA, www.rockland-inc.com), rabbit lysozyme (kindly provided by Dr. Tom Ganz), mouse αSMA and acetylated β-tubulin (Sigma, St. Louis, MO, www.sigmaaldrich.com), and rat ITGA6-APC (e-bioscience, San Diego, CA, www.ebioscience.com). The appropriate Alexa-Fluor coupled secondaries were used in double and triple staining sections. Sections were counterstained with DAPI (Vector labs - Burlingame, CA, www.vectorlabs.com) and analyzed by fluorescent microscopy with a Zeiss AxioImager microscope (Carl Zeiss, Jena, Germany, www.zeiss.com).

Separate Isolation of Mouse Tracheal SE and SMG

Mouse whole tracheas were dissected then cut below tracheal ring C4 into upper and lower parts. The lower part was processed for isolation of BCs as previously described [5] with modifications. Briefly, the lower two thirds of the tracheas were incubated for 30 minutes in 16 U/ml dispase (BD Biosciences, Bedford, MA, www.bdbiosciences.com) at room temperature, then for 20 minutes in 0.5 mg/ml DNase (Sigma). The epithelium was peeled off with forceps under a dissecting microscope, and then incubated in 0.1% trypsin for 20 minutes at 37°C to digest the peeled cell sheets into a single cell suspension. The upper parts were incubated in 0.15% pronase (Roche, Indianapolis, IN, www.roche.com) for 4 hours at 4°C. The remaining tracheal pieces were washed twice to ensure complete removal of all peeled SE. The remaining tracheal pieces were minced with a fine scissors for 5 minutes to open up the SMG compartments and incubated with pronase for 1 hour, then washed and incubated in 0.1% trypsin for 20 minutes at 37°C and passed through a 40-μm cell strainer to obtain a single cell suspension.

Fluorescence-Activated Cell Sorting

Cells from SE were stained for TROP-2 and ITGA6 conjugated to PE or APC (eBioscience and Biolegend) and cells from SMG were stained for TROP-2 by incubation with the antibody for 15 minutes at room temperature followed by washing and incubation in donkey anti-goat Alexa Fluor 488 or PE. Sorting was performed on a Fluorescence-Activated Cell Sorting (FACS) Aria and the data analyzed with FACS Diva software (BD Biosciences).

In Vitro Sphere Cultures

FACS-sorted cells were resuspended in mouse tracheal epithelial cells (MTEC)/Plus media [15], and mixed 1:1 with growth factor-reduced matrigel (BD Biosciences) [5]. The number of spheres per insert was counted on day 7. After 21 days in culture, spheres were embedded in Histogel and then in paraffin.

RNA Extraction and Amplification and Microarray Hybridization

Total RNA was extracted from sorted cell populations using RNeasy kits (Qiagen, Valencia, CN, www.qiagen.com) per the manufacturer's protocol. Amplification of RNA and subsequent microarray hybridization was performed following standard Affymetrix protocols.

Gene Expression Analysis

Raw gene expression data (.cel files) were generated by standard Affymetrix protocols and deposited in the Gene Expression Omnibus of the National Center for Biotechnology Information (accession number GSE28651). The import and normalization of the raw data were completed by Bioconductor in the R software environment. Two types of statistical tests (*t* test and rank product) were performed for each probe set to detect differentially expressed genes between the BCs and the duct cells. For both methods, only genes with an adjusted *p*-value <0.01 and fold change >=2 based on the false discovery rate were considered as differentially expressed genes and were annotated. Gene expression patterns of highly differentially expressed genes (the top 100 genes derived from the rank product methods) were compared by the heatmap function in R. We used the Database for Annotation, Visualization and Integrated Discovery [16] and the ingenuity pathways analysis database (Ingenuity Systems, http://www.ingenuity.com) to analyze biological functions and pathways of these highly differentially expressed genes.

Lineage Tracing

For lineage tracing experiments, 5–8-week-old mice hemizygous for *KRT14-CrePR1* and homozygous for *Rosa26-YFP*, received intratracheal injections with 500 μg RU486 in 25 μl of 20% acetone/80% sunflower oil using 0.3 ml insulin syringes (BD). Control mice received injections of only acetone/oil. Six days later, the mice were euthanized and their tracheas were collected, immersed in RU486 for 10 minutes and then transplanted heterotopically, as described above.

Statistics

All experiments were performed with at least three different primary cultures or mice in independent experiments. Significance was evaluated by Student's *t* test. Data are presented as mean ± SD.

Results

Identification of Large Airway Epithelial Cell Types that Survive a Severe-Hypoxic Ischemic Injury

The syngeneic, heterotopic murine tracheal transplant model results in interruption of the blood supply and causes a severe hypoxic-ischemic injury. In this model, complete in vivo regeneration of the trachea SE, SMGs, and SMG ducts occurs within 2–3 weeks [12, 13]. We hypothesized that the epithelial cells that survived this injury would be the stem/progenitor cells responsible for airway epithelial repair and regeneration. Extensive injury was seen on day 1 that reached its maximum on day 3 post-transplantation, as most of the SE and SMG cells sloughed off into the tracheal and ductal lumens and large areas of the basement membrane were denuded (Fig. 1Bii). Widespread expression of Annexin V, a marker of cell death, was seen in the SE and SMGs (Fig. 1Biii). In the SMGs, MECs, as well as mucus and serous tubules all became atrophic forming anuclear halos. The only cells that survived this injury were the K5+K14+ SMG duct cells and occasional K5+K14- BCs (Fig. 1Bii, iii).

The significant repair from only a few viable cells that was seen in this injury/repair model implies that these surviving cells contain the stem/progenitor cell populations for regenerating the pseudostratified SE, SMGs, and SMG ducts. As the only surviving epithelial cell populations in this model were some BCs and the SMG duct cells, we sought to characterize and compare the self-renewal and differentiation potential of each of these cell populations.

Development of a Strategy to Sort SMG Duct Cells Separately from BCs

To find specific markers to isolate the SMG duct cell population separately from the BC population, we first performed immunofluorescent staining for known markers of epithelial cell populations in the trachea. We found that the previously described [5] markers of airway BC, NGFR, and ITGA6, were expressed in both BCs as well as SMG duct cells, but were not expressed in MECs or tubule cells of the SMGs (Fig. 2Ai and ii). EpCAM was expressed on all epithelial cells of the airway (Fig. 2Aiii). TROP-2, a previously described marker of prostate BCs, [17], was expressed on all cells of the SE as well as the duct cells, but not in MECs or tubule cells of the SMGs (Fig. 2Aiii and iv).

On the basis of the pattern of TROP-2 expression, we decided to use enzymatic digestion of the trachea to completely remove the SE, including all BCs, followed by FACS sorting of the remaining trachea for TROP-2+ duct cells, thus excluding SMG tubular, MEC and nonepithelial stromal cells. Previous studies have used overnight protease XIV (pronase) [2, 9, 18] or 30 minutes of dispase [5] enzyme digestion to strip the SE from the rest of the

tracheal tissues. We performed a time course of digestion of the tracheal epithelium with pronase and found that 4 hours of digestion with pronase removed the SE without removing duct cells. However, longer time points of 8, 12, and 16 hours all removed duct cells in addition to BCs (Supporting Information Fig. S1).

We therefore exposed the upper third of mouse tracheas to 4 hours of pronase digestion to selectively remove the SE with the BCs, and then performed FACS of the single cell suspension obtained from the remaining tracheal tissue, using a primary antibody for the surface marker, TROP-2 (Fig. 2Bi). We found that 20% of total tracheal cells, after removing the SE, expressed TROP-2 and represented duct cells (Fig. 2Bi).

We found that SE collected from the trachea using pronase could not be used for BC sorting as it removed the surface epitopes of ITGA6 and NGFR preventing their use in FACS. We therefore performed tracheal digestion with dispase, but found that just 30 minutes was sufficient to strip not only the SE, but also considerable parts of the SMG ducts and tubules (Supporting Information Fig. S2). Therefore, as SMGs in mice are only present in the upper third of the mouse trachea [8], we used dispase digestion of only the lower two thirds of mouse tracheas to remove the SE to obtain a single cell suspension for FACS, specifically for BCs, using TROP-2 and ITGA6 (Fig. 2Bii). We found 35% of SE cells were TROP-2+ITGA6+ BCs.

In Vitro Self-Renewal and Differentiation Assays Comparing TROP-2+ Duct Cells and Basal Cells

To assess the ability of TROP-2+ duct cells to self-renew and differentiate in vitro, we used the three-dimensional sphere-forming assay that has been described for stem cells from the brain [19], prostate [17], distal lung [20, 21], and airway BCs [5]. TROP-2+ duct cells that were plated in matrigel produced an overall efficiency of colony formation of 0.67% ± 0.25% when duct cells where plated anywhere in the range of 10,000–60,000 cells per well. Two different morphologic types of TROP-2+ duct spheres were seen after 21 days in culture. The first consisted of a dense ball of cells with little or no central lumen. The second had a large central lumen with two to three cell layers lining the sphere, which were reminiscent of BC-derived tracheospheres [5] (Fig. 3Ai, ii). The size of the spheres varied from 50 to 300 μm with the spheres with larger lumen size being typically wider in diameter. Of the two types of spheres, 95% were dense spheres, and 5% were luminal spheres. To assess clonality, TROP-2+ duct cells from ubiquitously expressing GFP mice (β-actin-GFP, Jackson Labs) and wild-type mice were mixed 1:1 and colonies were examined for expression of GFP. The cells making up an individual colony were either all GFP+ or all wild-type confirming that these colonies are clonally derived from a single TROP-2+ duct cell, rather than by aggregations of sorted cells, which would give rise to mixed color colonies (Fig. 3Aiii). Control TROP-2 negative cells from the tracheas that contained the epithelial tubular cells, MECs, and stromal cells did not generate spheres in culture.

TROP-2+ITGA6+ BCs sorted from the lower two thirds of the tracheal SE, to ensure no contamination with duct cells, produced a clonal efficiency of 2.1% ± 0.6% when plated in the range of 10,000–60,000 cells per well. These cells differentiated into only the luminal type of spheres (Fig. 3Av, vi) and these spheres were also clonal (Fig. 3Avii). TROP-2+ITGA6- FACS-sorted cells did not form spheres.

To determine the differentiation ability of the TROP-2+ duct cells we examined expression in the spheres for proteins characteristic of differentiated cell types of the SE and the SMGs and ducts. Dense spheres from SMG duct cells, expressed K5 and K14 (Fig. 3Bi). The spheres also expressed K15, but did not express tubulin, SCGB1A1, or αSMA (Fig. 3Bii).

K8 was expressed in the cells in the center of the dense spheres in 48.25% ± 26% of spheres (Fig. 3Biii). Dense spheres demonstrated two patterns of p63 expression; one pattern showed nuclear p63 expression was only present in the basal layer of the sphere and in the other pattern it was expressed in all the cells of the dense sphere (Fig. 3Biv, v). A subset of the dense spheres (13.3% ± 5.1%) also expressed the serous cell marker, pIgR (Fig. 3Bvi) and there were spheres that stained positively for the mucus stain, AB/PAS (8.33% ± 8.28%) (Fig. 3Aiv). TROP-2 was expressed on all cells of the dense spheres (Fig. 3Bvii). The SMG duct cell spheres have been passaged up to four times and have the same efficiency of sphere formation, the same dense sphere morphology and equivalent differentiation ability.

FACS-sorted BCs produced spheres with a basal layer of K5 and K14 expressing cells (Fig. 3Bviii). K15, luminal K8, and nuclear p63 expression was also seen (Fig. 3Bix, x, and xi). BC spheres expressed tubulin in 60% ± 11.52% of spheres (Fig. 3Bxii) and a subset of the BC spheres expressed the serous cell marker, pIgR (56.2% ± 25.2%) (Fig. 3Bxii). The BC spheres did not express SCGB1A1 or αSMA. TROP-2 was present in all cells of the basal spheres (Fig. 3Bxiii). A subset of basal spheres produced mucus as detected by AB/PAS (28.5 ± 7.39) (Fig. 3Aviii).

The duct luminal spheres and the basal luminal spheres therefore had very similar differentiation capabilities, but duct luminal spheres did not differentiate into ciliated cells, unlike basal luminal spheres. We further compared the differentiation potential of duct and BCs in air-liquid interface cultures and found that they had very similar potential to form mucus and serous cells and that in this system duct and BCs had the same potential to differentiate into ciliated cells (Supporting Information Fig. S3).

Transcriptional Profiles of SMG Duct Cells and Basal Cells

We extracted RNA from FACS-sorted cells from TROP-2+ SMG duct tracheal cell populations as well as SE TROP-2+ITGA6+ tracheal BCs. RNA from the two populations was analyzed on the Affymetrix microarray platform. Of the 45,101 genes profiled in the gene expression data, 788 probes representing 776 genes with false discovery rate (FDR)-adjusted p-value of <0.01 and fold change ≥2 were identified as being differentially expressed between the BCs and the duct cells by the t test. Among these 776 genes, 528 (68%) were upregulated and 248 (32%) were downregulated in the duct cells. We clustered and displayed the 100 most differentially expressed genes to demonstrate that their transcription profiling patterns are substantially different between the BCs and the duct cells, while their patterns are quite similar within replicates (Fig. 4A). In addition, we adopted a nonparametric statistical method (the Rank Product) to the same data set and identified 74 differentially expressed genes (adjusted p-value <0.01 and fold change >=2). We found that these 74 differentially expressed genes belong to a subset of the 788 significant genes. Pathway analysis revealed enrichment in genes in duct cells compared with BCs that were related to epithelial development and more specifically to the development of stratified squamous epithelium, such as the skin. Such genes include the stratified epithelium-related gene cluster, termed the stratified epithelium secreted peptides complex, which harbors at least three genes encoding for the secreted peptides, dermokine (*Dmkn*), keratinocyte differentiation-associated protein (*Krtdap*), and suprabasin (*Sbsn*). One pathway was identified with genes that were upregulated in the SMG duct compared with BCs that are associated with dermatologic conditions and diseases and genetic disorders (Fig. 4B). Some genes of interest from this pathway included desmoglein (*Dsg1*), a core component of desmosomes, and insulin-like growth factor binding protein-4 (*Igfbp4*).

We also compared the transcription profiles of the BCs in this study to those of a population of FACS isolated lectin+; KRT5-GFP+ BCs in a previous study [5] and found that they were similar (Pearson's correlation coefficient of 0.851).

We performed quantitative real-time polymerase chain reaction (PCR) of some candidate genes found to be differentially expressed in basal and duct cells and confirmed that *K5*, *K14*, *Igfbp4*, and *Asprv1* have significantly higher expression in duct than in BCs ($p < .005$) (Fig. 4C). Immunostaining for IGFBP4 and ASPRV1 followed the same pattern of increased protein expression in duct compared with BCs (Fig. 4D).

Novel in Vivo Assay for Self-Renewal and Differentiation of SMG Duct Cells

To create an in vivo model of self-renewal and differentiation of airway epithelial stem/progenitor cells, we sought to recapitulate other in vivo adult stem cell model systems such as the mammary fat pad and renal capsule models [22–24]. We injected sorted TROP-2+ duct cells from RFP transgenic mice, into the fat pad around a recipient wild-type mouse scapula. We found that in 50% of the injected mice, SMG duct cells could organize themselves into SMG tubule-like structures (Fig. 5i and iii) that were RFP+ (i.e., of donor origin, Fig. 5i). These structures expressed K5 and K14 (Fig. 5ii and v) and were functional tubules as they expressed the serous cell marker lysozyme (Fig. 5vi) and mucus with positive staining for AB/PAS (Fig. 5iv). In addition, these SMG tubule-like structures contained αSMA and K14 expressing cells in a pattern consistent with the development of MECs (Fig. 5v and vi). In 20% of these grafts SMG duct-like structures were seen in addition to the typical SMG tubule-like structures (Fig. 5ii). This indicates that SMG duct cells can reconstitute functional SMG-like structures in vivo and that placing single duct cells in the dorsal fat pad niche represents a novel model to study the regeneration of SMG tubules and ducts.

In Vivo Lineage Tracing of Mouse Tracheal K14-Expressing Cells

In naïve mouse tracheas, cells that express K14 are only located in the SMG ducts and MECs, while less than 10% of SE BCs express K14 (Figs. 6i and [14]). To examine whether SMG duct cells participate in regenerating the SE, we performed lineage tracing of K14+ cells in transgenic mouse tracheas. We used a transgenic mouse model that selectively induces yellow fluorescent protein (YFP) expression in K14+ cells. K14CrePR1 mice [25] were bred with C57/BL6 ROSA26-floxSTOP-YFP mice (Jackson Labs). Because steady-state tracheal epithelial turnover is known to be very slow, we performed the lineage tracing using the same hypoxic-ischemic injury model we described above.

RU486 or vehicle control was administered intratracheally as previously described [25] on day 0. On day 6, tracheas were harvested from these transgenic mice and immersed in RU486 or vehicle control, before being transplanted heterotopically into syngeneic wild-type recipient mice. The tracheal transplants were harvested 7 days later and immunostaining was performed for YFP and K14 expression. The timing of the dosing of RU486 was such that only the surviving K14+ duct cells and the few K14+ BCs of the steady-state SE would have been subject to induction of Cre-recombinase and therefore expression of YFP. Cells that turned on K14-expression as part of the repair process would therefore not have been exposed to RU486 and induction of Cre-recombinase. Vehicle control treated tracheas did not show any evidence of YFP expression. At 7 days post-transplantation, YFP expression was found in the SMGs, SMG ducts and the SE adjacent to and overlying the SMG ducts (Fig. 6ii and iii). In the lower two thirds of the trachea, which does not have SMGs, a few randomly scattered foci of YFP+K14+ cells were seen in the SE (Fig. 6iv) likely reflecting induction of YFP expression in a few K14+ BCs. Quantification of YFP+ SE derived from K14+ SMG duct cells demonstrated that SMG duct cells gave rise to 25%–30% of the airway epithelium of the upper third of the trachea. By comparison, the YFP+ SE only represented <5% of the tracheal surface area in the lower two thirds of the trachea. This indicates that SMG duct cells do participate in repairing the SE in the presence of BCs.

Discussion

Our data show that SMG duct cells are a population of multi-potent stem/progenitor cells that survive a severe hypoxic-ischemic injury in the tracheal epithelium and play a role in repair of the SMGs, SMG ducts and SE analogous to the identification of stem cell populations in the ducts of other tissues [10, 11]. We developed a novel method to isolate SMG duct cells by FACS and used in vitro and in vivo models of stem/progenitor cell self-renewal and differentiation to compare the regenerative potential of known stem/progenitor cells in the airway SE, namely the BCs, to the SMG duct cells. We found that unlike BCs, SMG duct cells were capable of repairing the SMG serous and mucus tubules and MECs and that they were also able to regenerate SE. We speculate that previous reports of surface airway epithelial cell and BC self-renewal and differentiation ability may have been affected by enzymatic digestion methods that also allowed duct cells to be included with BC preparations [2, 5, 18, 26]. This likely explains why air-liquid interface cultures from the proximal half of the mouse trachea are more efficient at making airway epithelium than the distal half, which has no SMGs and ducts, but both halves are capable of generating differentiated airway epithelium in culture [15]. We believe that our data demonstrate that BCs and duct cells both contain stem/progenitor cells, but that within duct cells there is a more multipotent stem/progenitor cell.

We found important similarities and differences between the SMG duct stem/progenitor cell population and the BC stem/progenitor population. The SMG duct cells are distinct from the BCs in that (a) they give rise mostly to dense clonal spheres in culture, (b) they are capable of generating SMG-like structures in an in vivo model of regeneration, (c) lineage tracing shows that this population forms SMGs, SMG ducts, and SE adjacent to the SMG ducts, and (d) microarray analysis demonstrates key differences in the nature of the epithelium of the duct cells as compared with BCs. However, there are also similarities between the SMG duct and BC stem/progenitor populations: (a) they both express the surface markers ITGA6 and NGFR and (b) in the sphere-forming and air-liquid interface assays, they have similar differentiation capacity.

SMG duct cells express K14 and we showed previously that under steady-state conditions, only 10% of mouse BCs and just 1% of human BCs of the SE express K14 [14]. However, premalignant lesions of the SE all express K14 and the presence of K14 in primary non-small cell lung cancer (NSCLC) tissue was associated with a poor prognosis [14]. The presence of K14 in the airway epithelium therefore appears to correlate with response to injury and the presence of stratified rather than pseudostratified epithelium. The microarray gene expression profile comparison of SMG duct and BCs demonstrates that the duct cells are programmed toward stratified squamous epithelium and express genes that are associated with stratified squamous epithelial cancers, such as squamous skin cancer. This leads us to speculate that SMG duct cells may be a stem cell of origin for NSCLC. We further hypothesize that because duct cells can give rise to glandular structures (the SMGs), as well as SE, that it is possible that they could give rise to NSCLCs with both squamous and adenocarcinoma histologies.

In mice, the SMGs and SMG ducts are only present in the upper third of the trachea [8] and the SMG duct cells, therefore, likely do not play the major role in repair of the airway epithelium. However, in other mammals such as pigs and humans, SMGs and SMG ducts are found throughout the cartilaginous airways and it is therefore possible that SMG ducts play a larger role in repair of the airway SE, in addition to repair of the SMGs and SMG ducts after injury in humans. There are a number of clinical scenarios where injury results in sloughing of the SE, for example in respiratory syncytial virus infection or acute smoke

inhalation. We envision that the SMG duct cells will play an important role in repair of the airway epithelium in these situations.

A normal human bronchial epithelial cell line (Clonetics Cell Systems, Lonza, Walkersville, MD) has been shown to generate spheres and possess self-renewal and differentiation potential in matrigel cultures [27]. These spheres were able to differentiate to mucus and serous cell types and produced luminal spheres in culture. However, it is not clear whether SMG duct cells might be included in the culture system, as the nature of the human samples used to generate these cell lines is proprietary information. On the basis of our studies, it seems likely that SMG duct cells as well as BCs are included in these cell preparations.

A similar strategy of lineage tracing K14-expressing cells in the airway has been recently published [28]. Although the investigators did not focus on SMGs or SMG ducts, they did comment that they detected cells derived from K14+ cells in the SMG tubules and ducts but not in the SE adjacent to the glands. Two aspects of this previous study hampered the investigators' ability to assess the role of SMG ducts in repair and regeneration of the airway epithelium. Firstly, the authors found that endogenous B-galactosidase activity was present in peritracheal glands and they could therefore not perform lineage tracing in these areas. Secondly, the naphthalene model of airway epithelial injury used in the study is not as severe an injury as the hypoxic-ischemic tracheal transplant model and may not therefore require the recruitment of SMG duct cells for repair of the SE.

We found that SMG duct cells have approximately a fourfold lower colony generating capacity than BCs. There are a number of possible explanations for this. One major reason is that SMG duct cells are comprised of at least three distinctive cell populations, namely, BCs of the duct (ITGA6+/NGFR+/tubulin−), ciliated cells of the duct (ITGA6−/NGFR−/tubulin +), and nonciliated, non-BCs of the duct (ITGA6-/NGFR−/tubulin−). It is possible that only one of these cell populations is the genuine stem/progenitor cell and thus with our current method of sorting all TROP-2+ duct cells, we are only obtaining a population that is enriched for the true duct stem/progenitor cell. Another possible explanation is that SMG duct cells are in a more protected location and not exposed to constant environmental injury, as the BCs are. They, therefore, only need to be recruited for repair in the setting of a severe injury and so may cycle more slowly.

Recently, a stem cell was identified in the lung that appears to have the potential to differentiate into a number of different cell types of the proximal and distal airway epithelium as well as into the lung vasculature [29]. If this work can be replicated, then it suggests that there is a lineage hierarchy in the lungs and that duct cells are considerably further down the lineage than these lung stem cells.

Conclusion

We have identified a novel multipotent stem/progenitor cell in the SMG duct in the airway epithelium. This is of major importance to the field of lung regeneration. SMG hypertrophy is associated with airway inflammation and excessive mucus secretions, which are frequently seen in patients with chronic asthma, chronic obstructive pulmonary disease, and cystic fibrosis [1]. Our ability to identify the SMG duct cells and their regenerative ability has implications for the possible identification of novel therapeutic targets for airway diseases and potential cell-based therapies in the future.

Acknowledgments

We would like to acknowledge the UCLA Clinical Microarray Core and the Broad Stem Cell Research Center Fluorescence-Activated Cell Sorting Core. We would like to thank Jessica Scholes and Felicia Codrea for their help

with cell sorting. We would like to thank Dr. Gay Crooks for her help with the manuscript. We would also like to acknowledge Xiao Jing Wang who provided us with the K14CrePR1 mice. This work was supported by CIRM RN2-00904-1, K08 HL074229, American Thoracic Society/Chronic Obstructive Pulmonary Disease Foundation ATS-06-065, The Concern Foundation, The UCLA Jonsson Comprehensive Cancer Center Thoracic Oncology Program/Lung Cancer specialized program of research excellence (SPORE), the University of California Cancer Research Coordinating Committee, and the Gwynne Hazen Cherry Memorial Laboratories (B.G.).

References

1. Bartlett JA, Fischer AJ, McCray PB Jr. Innate immune functions of the airway epithelium. Contrib Microbiol. 2008; 15:147–163. [PubMed: 18511860]
2. Schoch KG, Lori A, Burns KA, et al. A subset of mouse tracheal epithelial basal cells generates large colonies in vitro. Am J Physiol Lung Cell Mol Physiol. 2004; 286:L631–L642. [PubMed: 12959927]
3. Hong KU, Reynolds SD, Watkins S, et al. In vivo differentiation potential of tracheal basal cells: Evidence for multipotent and unipotent subpopulations. Am J Physiol Lung Cell Mol Physiol. 2004; 286:L643–L649. [PubMed: 12871857]
4. Hong KU, Reynolds SD, Watkins S, et al. Basal cells are a multipotent progenitor capable of renewing the bronchial epithelium. Am J Pathol. 2004; 164:577–588. [PubMed: 14742263]
5. Rock JR, Onaitis MW, Rawlins EL, et al. Basal cells as stem cells of the mouse trachea and human airway epithelium. Proc Natl Acad Sci USA. 2009; 106:12771–12775. [PubMed: 19625615]
6. Rawlins EL, Okubo T, Xue Y, et al. The role of Scgb1a1+ Clara cells in the long-term maintenance and repair of lung airway, but not alveolar, epithelium. Cell Stem Cell. 2009; 4:525–534. [PubMed: 19497281]
7. Meyrick B, Sturgess JM, Reid L. A reconstruction of the duct system and secretory tubules of the human bronchial submucosal gland. Thorax. 1969; 24:729–736. [PubMed: 5350723]
8. Rawlins EL, Hogan BL. Intercellular growth factor signaling and the development of mouse tracheal submucosal glands. Dev Dyn. 2005; 233:1378–1385. [PubMed: 15973734]
9. Borthwick DW, Shahbazian M, Krantz QT, et al. Evidence for stem-cell niches in the tracheal epithelium. Am J Respir Cell Mol Biol. 2001; 24:662–670. [PubMed: 11415930]
10. Visvader JE. Keeping abreast of the mammary epithelial hierarchy and breast tumorigenesis. Genes Dev. 2009; 23:2563–2577. [PubMed: 19933147]
11. Kimoto M, Yura Y, Kishino M, et al. Label-retaining cells in the rat submandibular gland. J Histochem Cytochem. 2008; 56:15–24. [PubMed: 17875657]
12. Gomperts BN, Belperio JA, Rao PN, et al. Circulating progenitor epithelial cells traffic via CXCR4/CXCL12 in response to airway injury. J Immunol. 2006; 176:1916–1927. [PubMed: 16424223]
13. Genden EM, Iskander A, Bromberg JS, et al. The kinetics and pattern of tracheal allograft re-epithelialization. Am J Respir Cell Mol Biol. 2003; 28:673–681. [PubMed: 12760965]
14. Ooi AT, Mah V, Nickerson DW, et al. Presence of a putative tumor-initiating progenitor cell population predicts poor prognosis in smokers with non-small cell lung cancer. Cancer Res. 2010; 70:6639–6648. [PubMed: 20710044]
15. You Y, Richer EJ, Huang T, et al. Growth and differentiation of mouse tracheal epithelial cells: Selection of a proliferative population. Am J Physiol Lung Cell Mol Physiol. 2002; 283:L1315–L1321. [PubMed: 12388377]
16. Huang Da W, Sherman BT, Lempicki RA. Systematic and integrative analysis of large gene lists using DAVID bioinformatics resources. Nat Protoc. 2009; 4:44–57. [PubMed: 19131956]
17. Goldstein AS, Lawson DA, Cheng D, et al. Trop2 identifies a subpopulation of murine and human prostate basal cells with stem cell characteristics. Proc Natl Acad Sci USA. 2008; 105:20882–20887. [PubMed: 19088204]
18. Engelhardt JF, Yankaskas JR, Wilson JM. In vivo retroviral gene transfer into human bronchial epithelia of xenografts. J Clin Invest. 1992; 90:2598–2607. [PubMed: 1281842]
19. Reynolds BA, Weiss S. Generation of neurons and astrocytes from isolated cells of the adult mammalian central nervous system. Science. 1992; 255:1707–1710. [PubMed: 1553558]

20. McQualter JL, Yuen K, Williams B, et al. Evidence of an epithelial stem/progenitor cell hierarchy in the adult mouse lung. Proc Natl Acad Sci USA. 2010; 107:1414–1419. [PubMed: 20080639]

21. Inayama Y, Hook GE, Brody AR, et al. The differentiation potential of tracheal basal cells. Lab Invest. 1988; 58:706–717. [PubMed: 3379917]

22. Xin L, Ide H, Kim Y, et al. In vivo regeneration of murine prostate from dissociated cell populations of postnatal epithelia and urogenital sinus mesenchyme. Proc Natl Acad Sci USA. 2003; 100(suppl 1):11896–11903. [PubMed: 12909713]

23. Vu TH, Alemayehu Y, Werb Z. New insights into saccular development and vascular formation in lung allografts under the renal capsule. Mech Dev. 2003; 120:305–313. [PubMed: 12591600]

24. Shackleton M, Vaillant F, Simpson KJ, et al. Generation of a functional mammary gland from a single stem cell. Nature. 2006; 439:84–88. [PubMed: 16397499]

25. Malkoski SP, Cleaver TG, Lu SL, et al. Keratin promoter based gene manipulation in the murine conducting airway. Int J Biol Sci. 2010; 6:68–79. [PubMed: 20140084]

26. Engelhardt JF, Schlossberg H, Yankaskas JR, et al. Progenitor cells of the adult human airway involved in submucosal gland development. Development. 1995; 121:2031–2046. [PubMed: 7635050]

27. Wu X, Peters-Hall JR, Bose S, et al. Human bronchial epithelial cells differentiate to 3D glandular acini on basement membrane matrix. Am J Respir Cell Mol Biol. 2011; 44:914–921. [PubMed: 20724555]

28. Ghosh M, Brechbuhl HM, Smith RW, et al. Context-dependent differentiation of multipotential keratin 14-expressing tracheal basal cells. Am J Respir Cell Mol Biol. 2010

29. Kajstura J, Rota M, Hall SR, et al. Evidence for human lung stem cells. N Engl J Med. 2011; 364:1795–1806. [PubMed: 21561345]

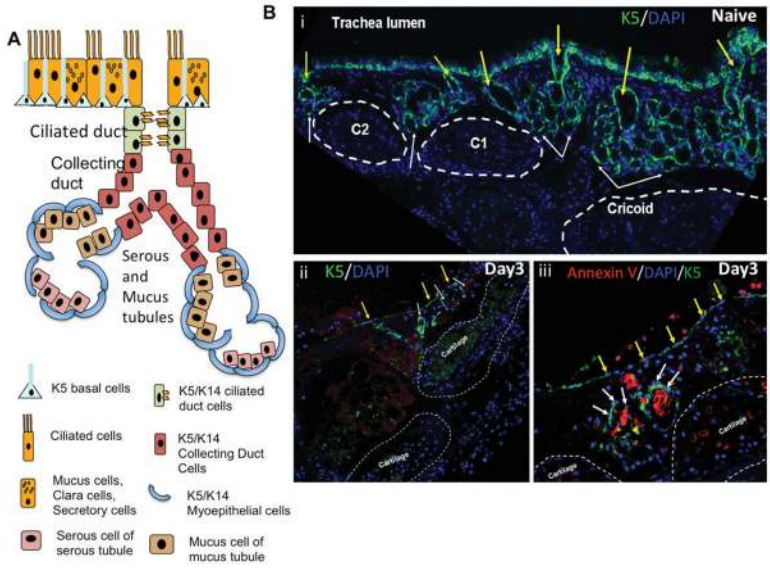

Figure 1.

Location of cell types of the cartilaginous airways. **(A):** Schematic of the airway epithelial cell types of the cartilaginous airways. **(B):** A few basal cells (BCs) and submucosal gland (SMG) duct cells are the only cells that survive the hypoxic-ischemic injury. Syngeneic heterotopic murine tracheal transplantation was performed, and transplanted tracheas were collected and examined on day 3 when there is maximal cell death. ($n = 4–6$ tracheas per time point). A longitudinal section of a naïve trachea immunostained with K5, demonstrates the pseudostratified surface epithelium (SE) and the SMG ducts (yellow arrows) of the upper trachea (i). Only SMG duct (white arrows) and a few scattered BCs on the SE survived the hypoxic-ischemic injury. Wide areas of the basement membrane (BM) were denuded and the few cells that remained attached to the BM were K5 positive. SMG ducts were lined with K5+ cells while SMG tubules and myoepithelial cells were necrotic (ii, iii). Annexin V expression was seen in the sloughed cells in the lumen, SMG tubules and ducts (iii). Abbreviation: DAPI: 4′,6-diamidino-2-phenylindole.

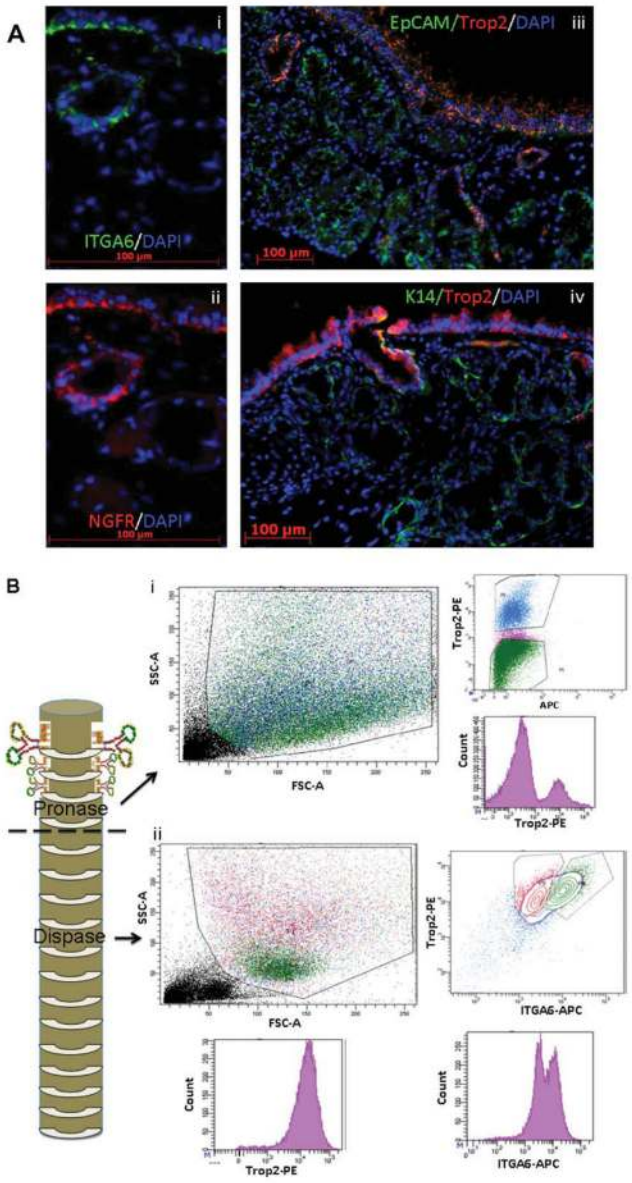

Figure 2.

Characterization and isolation of submucosal gland (SMG) duct cells. **(A):** Immunofluorescent staining of SMG duct cells with primary antibodies for specific surface markers. ITGA6 and NGFR are expressed in basal cells (BCs) and are also expressed in the SMG duct (i, ii). EpCAM is present on all epithelial cells of the surface epithelium (SE), SMG tubules, and SMG duct, but TROP-2 is expressed in the cells of the SE and SMG duct, but not in the SMG tubules (iii, iv). K14 is expressed in SMG duct cells, and myoepithelial cells of the tubules (iv). **(B):** Fluorescence-activated cell sorting of SMG duct and BC populations. (i) The scatter plot shows the distribution of the tracheal cells remaining after stripping of the SE, that is, SMG ducts, tubules and surrounding stroma. TROP-2+ duct cells (blue) and TROP-2- nonduct cells (green) were sorted. Duct cells represented 20% of the total cells. (ii) The scatter plot shows the distribution of the stripped tracheal surface epithelial cells. TROP-2+ITGA6+ BCs (green) and TROP-2+ITGA6- non-BCs (red) were sorted. BCs represented approximately 35% of the total cells. Abbreviations: APC:

Allophycocyanin; DAPI: 4′,6-diamidino-2-phenylindole; EpCAM: epithelial cell adhesion molecule; FSC-A: forward scatter; PE: Phycoerythrin; SSC-A : side scatter; TROP-2 : tumor-associated calcium signal transducer 2.

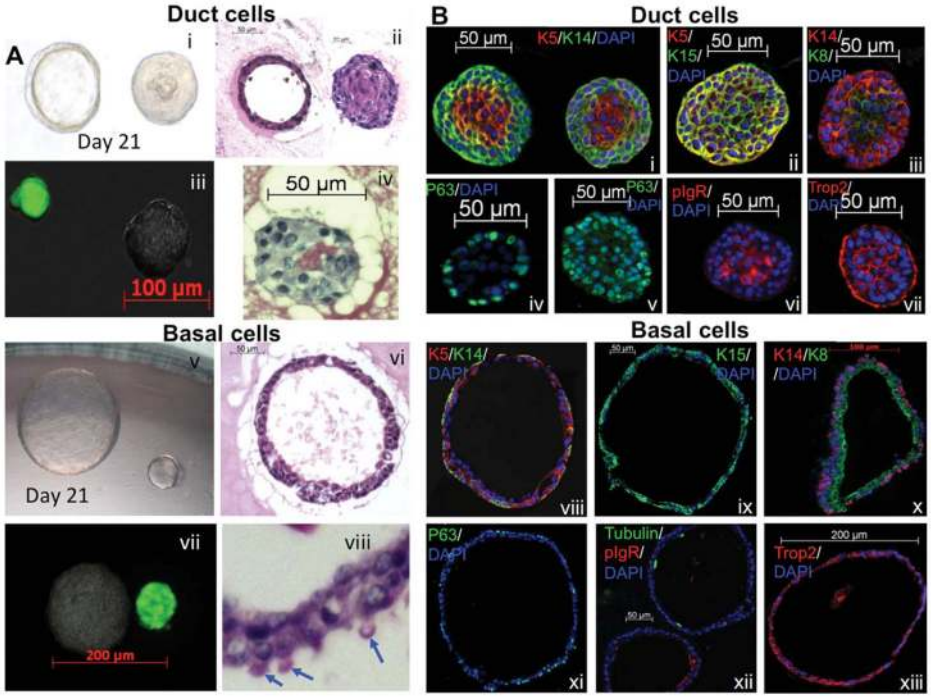

Figure 3.

In vitro self-renewal and differentiation ability of submucosal gland (SMG) duct cells compared with basal cells (BCs). **(A):** The sphere-forming assay: Sphere morphology, clonality, and ability to synthesize mucin. Sorted TROP-2+ SMG duct cells were capable of generating spheres in vitro. Morphologically, two different kinds of spheres were generated; luminal type spheres (i-left) and dense spheres with little or no lumen (i-right). The dense spheres were generally smaller in diameter than the luminal spheres and ranged in size from 20 to 100 μm. The luminal spheres raged from 50 to 300 μm. H&E of a cross-section of the spheres demonstrated the lack of a central lumen in the dense spheres as compared with the luminal spheres (ii). Mixed 1:1 ratio of GFP:wild-type-sorted duct cells demonstrated only green or wild-type spheres, indicating that spheres arose clonally from a single stem/progenitor cell (iii). Sorted duct cells produced mucus in the sphere cultures as seen by Alcian Blue/periodic acid-Schiff (AB/PAS) staining (iv). Sorted TROP-2+integrin-α-6+ BCs from the surface epithelium also generated spheres in vitro. Morphologically, there were just luminal spheres, which varied in size from 50 to 300 μm (v, vi). Mixed 1:1 ratio of GFP:wild-type-sorted BCs demonstrated only green or wild-type spheres, indicating that spheres arose clonally from a single stem/progenitor cell (vii). Sorted BCs produced mucus in the sphere cultures as seen by AB/PAS staining (viii). **(B):** The sphere-forming assay: Differentiation ability. Dense spheres from duct cells expressed K5 and K14 in all the cells of the sphere (i), with K5 being more strongly expressed on the outside (basal side) of the sphere, with K14 being strongly expressed on the inside (luminal side) of the sphere. K15 was expressed in all cells of the sphere (ii). The dense spheres expressed K8 (48.25% ± 26%) in a luminal pattern (iii). p63 was found in two patterns, either on the basal surface or throughout the dense sphere (iv, v). Spheres expressed the serous cell marker (13.3% ± 5.1%), pIgR (vi). TROP-2 was found on all cells of the sphere (vii). The basal spheres expressed K5 and K14 in almost all the cells of the sphere (viii). p63 was found in cells located on the periphery (xi) and 100% of the spheres expressed K8 in a central pattern (x). K15 was expressed equally in all cells of the sphere (ix). Spheres expressed the secretory marker (56.2% ± 25.2%), pIgR, and 60% ± 11.52% expressed the ciliated marker, acetylated β-tubulin (xii). TROP-2 was found on all cells of the spheres (xiii). Abbreviations: DAPI:

4′,6-diamidino-2-phenylindole; pIgR: polymeric immunoglobulin receptor; TROP-2: tumor-associated calcium signal transducer 2.

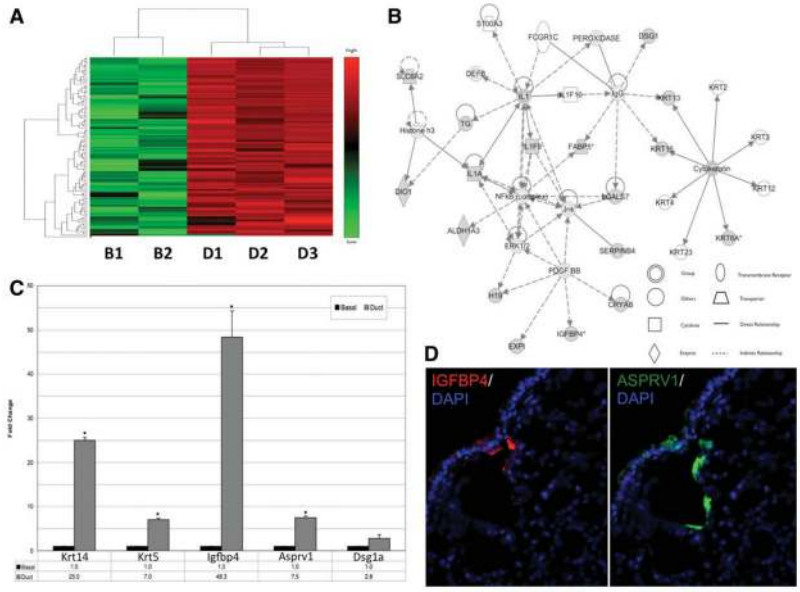

Figure 4.

Gene expression profiling of submucosal gland (SMG) duct cells compared with basal cells (BCs). **(A):** The heatmap shows the 100 most differentially expressed genes between sorted duct and BCs and demonstrates that their transcriptional profile is substantially different between the BCs and the duct cells, while their patterns are quite similar within replicates. **(B):** The ingenuity pathways analysis database was used to analyze biological functions and pathways of the 74 most highly differentially expressed genes. Pathway analysis revealed enrichment in genes in duct cells compared with BCs that were related to epithelial development, such as skin and hair development and dermatological conditions and diseases. **(C):** Validation of the microarray gene expression of candidate genes was performed with quantitative real-time PCR. *K14*, *K5*, *Igfbp4*, and *Asprv1* were more highly expressed in duct as compared with BCs. Data were analyzed using a two-tailed unequal variance Student's *t* test. Asterisk indicates a *p*-value <.005. *Dsg11* trended to significance with a *p*-value of 0.06. **(D):** Immunofluorescent staining of IGFBP4 and ASPRV1 in tracheal samples confirmed the location of these proteins was mostly in the SMG duct. ASPRV1 is also located in a few apical cells of the surface epithelium (SE) adjacent to the opening of SMG ducts on the SE. Abbreviations: ALDH1A3: aldehyde dehydrogenase 1A3; ASPRV1: aspartic peptidase, retroviral-like 1; CRYAB: crystallin, alpha B; DAPI: 4′,6-diamidino-2-phenylindole ; DEFB -beta defensin; DIO1: deiodinase, iodothyronine, type I; DSG1: desmoglein 1; ERK1/2: extracellular signal-regulated kinase 1/2; EXP1: exportin 1; FABP5: fatty acid binding protein 5; FCGR1C: Fc fragment of IgG, high affinity Ic, receptor; IGFBP4: insulin-like growth factor binding protein 4; IL1A: interleukin 1, alpha; JNK: c-Jun N-terminal kinase; KRT: keratin; LGALS7: lectin, galactose binding, soluble 7; NFKB: nuclear factor kappa-B; PDGF B: platelet derived growth factor, B polypeptide; SERPINB4: serpin peptidase inhibitor, clade B (ovalbumin), member 4; SLC6A2: solute carrier family 6 (neurotransmitter transporter, noradrenalin), member 2; TG: thyroglobulin.

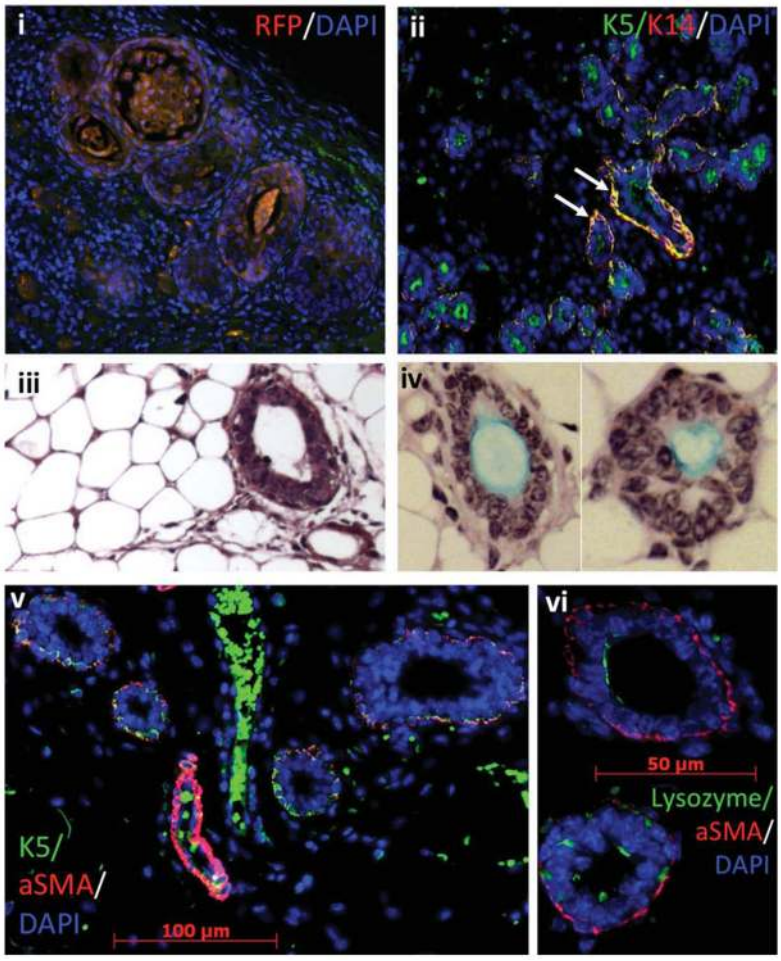

Figure 5.

Sorted RFP+TROP-2+ duct cells reconstitute submucosal gland (SMG) tubule-like and SMG duct-like structures in an in vivo regeneration model. To examine the ability of SMG duct cells to reconstitute SMG-like and SMG duct-like structures in vivo, we placed fluorescence-activated cell sorting-sorted RFP+TROP-2+ duct cells into the fat pad under the skin of the mouse back ($n = 20$, 5,000 cells per mice). We found that in 50% of the grafts, SMG duct cells could organize themselves into SMG tubule-like structures (i–v) and were RFP+, that is, of donor origin (i). These SMG-like structures were K5+ and K14+ (ii, v) and expressed the serous cell marker, lysozyme (vi). In 20% of grafts SMG duct-like structures were seen in addition to the typical tubule-like structures (arrows) (ii). Cells around the SMG tubule-like structures expressed K5 and αSMA, which are markers of myoepithelial cells (v, vi). Abbreviation: αSMA: α-smooth muscle actin.

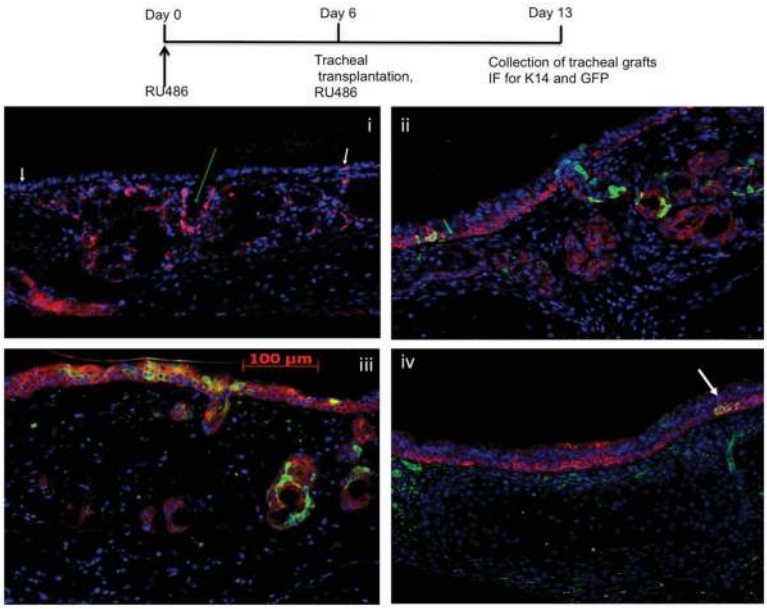

Figure 6.

Lineage tracing of K14-YFP-expressing cells in the in vivo tracheal transplant airway regeneration model after hypoxic-ischemic injury. In naïve mouse tracheas, cells that express K14 are almost entirely located in the submucosal gland (SMG) ducts (white arrow) and thin myoepithelial cells, and only 10% of surface epithelium (SE) basal cells express K14 (green arrow) (i). To trace the contribution of K14+ SMG duct cells to the repair of the airway epithelium after hypoxic-ischemic injury, we used a transgenic mouse model to selectively induce YFP expression in K14-expressing cells. K14CrePR mice [25] were bred with ROSA26-floxed STOP-YFP mice. RU486 or vehicle control was administered intratracheally on day 0. On day 6, tracheas were harvested from these transgenic mice and tracheas were immersed in RU486 or vehicle control, before being transplanted heterotopically into wild-type recipient mice. These tracheal transplants were harvested 7 days later and immunostaining was performed for YFP and K5 and K14 expression. YFP expression was found to colocalize with regions of K14 expression of the SMG, SMG duct and the SE adjacent to and overlying the SMG ducts (ii, iii). In the lower two thirds of the trachea, which does not have SMGs, a few randomly scattered foci of YFP+K14+ cells were seen in the SE (iv, arrow). Abbreviation: GFP: green fluorescent protein.